Oligomeric baroeffect and gas aggregation states

David A. Noever

NASA Marshall Space Flight Center, ES-76, Huntsville, Alabama 35812

The baroeffect is analyzed to include a gas that aggregates into higher-order polymers or oligomers. The resulting pressure change is found to vary independently of the molecular weight of the gas components and to depend only on the aggregation or oligomeric order of the gas. With increasing aggregation, diffusive slip velocities are found to increase. The calculations are extnded to include general counterdiffusion of two distinct aggregation states (k-, j-mer) for the gas, and the pressure change is derived as a function that is independent of both molecular weight and the absolute aggregation. The only parameter that determines the baroeffect is the ratio of aggregated states, $\beta = k/j$. For gases that reversibly aggregate, possible oscillatory behavior and complex dynamics for pressure are discussed. Gas aggregation may play a role for low-temperature crystal-growth conditions in which vapor concentrations of one (or more) species are high.

I. INTRODUCTION

The baroeffect [1–8] refers to a transient pressure gradient that develops during the isothermal diffusion of very different molecular weight gases. This measurable pressure increase arises locally from the faster molecular speed of a lighter gas relative to a heavy one, a result which leads to a short-term buildup of molecules in regions dense with the high molecular weight species. Heavy-gas regions become more concentrated with light species. As a consequence, a backflow or bulk gas motion can arise to correct for local pressure differences. This pressure increase (up to 10% of total pressure) can be substantial, both in normal [1,9] and Knudsen [2,3] diffusion regimes. The physics of this sequence—light gas moving faster, concentrating in regions rich in heavy gas and subsequent pressure corrections—mirrors many of the well-known solid-state phenomenon called anomalous diffusion or the Kirkendall effect [10,11]. In fact, McCarty and Mason [1] have referred to the preceding description of disparate molecular weight mixtures as a gas Kirkendall effect.

Both theoretically and experimentally, Kramers and Kistemaker [9] first treated the problem using two glass bulbs (one filled with heavy gas, the other light gas) connected by a capillary. Using this dumbbell configuration, they measured the pressure difference between the bulbs as a function of time and gas composition. What they found was that the experimental pressure gradients were not consistent with predictions of standard parabolic (Poisseiulle) flows in a capillary. Consequently, they proposed a modified theory which preserved their formal treatment, but loosened the traditional restriction of no-slip or stick boundary condition. In all but abnormal cases, the no-slip condition serves elsewhere as the phenomenological rule: fluid flow ceases at solid boundaries, the result of which is a bullet-shaped velocity profile. Kramers and Kistemaker called the loosened restriction a diffusive slip condition, owing to its measurable appearance in counterdiffusing gases. Subsequent workers [1–8] have verified their general picture for a variety of geometries and gas pairs.

While the experimental procedure that accompanies the baroeffect is well established, a number of outstanding theoretical issues remain. If, as in most other fluid cases, no-slip is the rule, why should this important condition break down in its multicomponent generalization? Perhaps more importantly, why should two gases ever yield no-slip (zero mass-averaged velocity), particularly given counterdiffusing fluxes of gases with strikingly different properties (molecular weight and thermal speeds, gas-gas and gas-wall interatomic potentials, etc.)? Regarding the latter issue, it is difficult to see why fluxes should *exactly* cancel to zero at a boundary for all materials and experimental conditions. This problem, how to generalize no-slip to multicomponent diffusion, has been recently acknowledged to remain somewhat of a physical mystery [12]. The significance of its solution arises directly in modeling mass transport of optical and electronic crystals grown from their multicomponent vapors [13–15]. If no-slip is not generally valid for these counterdiffusing mixtures, then the physics of closed vapor transport will require revision (Fig. 1). For example, computer models [13] that use no-slip predict substantial gas recirculation and convective rolls which arise from (or are driven by) the need for mass-averaged fluxes to vanish near a wall (no-slip). In this case, the boundary interaction would generate novel (and gravity-independent) mechanisms for convection.

As a starting point for investigating this potentially important effect, a series of limited generalizations has been tried [16]. Of note here is the case for three gases, one of which is uniformly distributed, that has presented some unique backflow regimes which, depending on the selected molecular weights, lead theoretically to pressure reversals from light *toward* heavy gas. This is opposite to the case for simple binary baroeffects and can become large for the right recipe of gas mixtures. This generalization
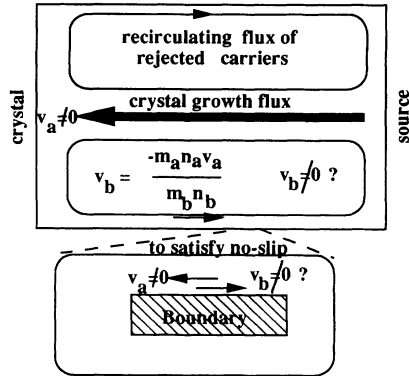
recirculating flux of
rejected carriers

crystal growth flux

$v_a \neq 0$ crystal   source

$v_b = \dfrac{-m_a n_a v_a}{m_b n_b}$ $v_b \neq 0$?

to satisfy no-slip

$v_a \neq 0 \longleftarrow \longrightarrow v_b \neq 0$?

Boundary

FIG. 1. Schematic of possible flow configuration in vapor transport. The net flux of a crystallizing gas a exists along the wall to satisfy the growth conditions near the crystal corners. If no-slip is applied, that the mass-averaged velocity vanishes at the wall, then a returning flux of a carrier gas b must exist to balance $n_a m_a v_a + n_b m_b v_b = 0$, $v_b = n_a m_a v_a / n_b m_b$. This sets conditions for recirculation driven by a wall interaction; see text.

was called the ternary baroeffect. In a further refinement, the present work treats a single gas species which can exist in two different aggregation states. These aggregation states are oligomeric, consisting of monomers, dimers, etc. of the same gas. Experimental evidence for such aggregation states exists at low temperatures (near the gas condensation point) [17–22]. For these conditions, molecular clustering is more common than not and thus the single-species oligomeric baroeffect is worth investigating here to understand further the significant points (and to ignore irrelevant ones) in gas flows near a wall. To anticipate the result, the analysis yields a particularly appealing form for the calculated pressure difference, one which depends on the relative degree of aggregation or oligomeric order.

II. DEFINITION OF NEAR-WALL GAS VELOCITY

The theory treats the isothermal counterdiffusion of two aggregated gases moving from opposite ends of a capillary. Its aim is to derive pressure relations and velocities as a function of gas properties; the usual property varied in gas molecular weight. Much of the motivation underlying the various steps in the calculation has appeared elsewhere [23,24] and will not be repeated in detail. The important physical idea turns on a distinction between at least four types of gas velocities: (i) the random thermal speed c, which follows from simple kinetic theory $c = (kT/m)^{1/2}$, where T is temperature (K), m is molecular mass, and k is Boltzmann's constant; (ii) the individual diffusion velocities v_i for component i in the mixture; (iii) the mass-averaged diffusion velocity for the bulk mixture $v_m = \sum_i m_i n_i v_i / \sum_i m_i n_i$, where each summation $\sum_i$ is carried over all species i with mole number n_i; and finally (iv) the near-wall gas mixture (flow) velocity $v_w = v_m - v_s$, where v_s is the slip velocity linearly extrapolated from the bulk directly to the solid boundary. These (myriad) definitions of velocity are important descriptions and as has been noted previously, have led to some his-

torical confusion [23]. The formalism adopted here owes its origin to Kramers and Kistemaker's first remarks [9] and deserves further explanation only for defining an appropriate wall velocity. What does it mean to speak of the near-wall gas velocity v_w?

The significance of v_w to Kramers's theory traces back to Maxwell [25], who conceded that near a boundary the reduced number of gas-gas collisions and increased number of gas-wall collisions posed a problem to kinetic theory. A complete theory requires two items, a solution for the gas velocity distribution (non-Maxwellian) and an appropriate hypothesis (or guess) as to what collision function best fits with velocity boundary conditions on a Boltzmann equation (momentum conservation with collisions). However, for all but simple collision integrals, the general Boltzmann equation cannot be solved with difficult or realistic boundary conditions. Kramers and subsequent workers have opted instead for a lowest-order approximation to the velocity boundary condition: the slip velocity v_s appears as a *linear extrapolation* of the mass-averaged velocity v_m and the near-wall velocity v_w taken a few mean free paths into the bulk and away from the boundary. This lowest-order approximation defines the gas velocity v_s at the boundary. Alternative ways to put together a coherent picture of slip velocity have appeared, namely those which define a flux along the boundary as a kind of surface diffusion [24]. In the spirit of a first-order investigation, this work will adopt Kramers and Kistemaker's original definition to compare oligomeric effects with previous calculations.

With these preliminaries, the method is relatively straightforward: write component velocities which reflect a gas's relative degree of aggregation (oligomeric order) and solve for the resulting mass-averaged and near-wall velocities. These velocities yield a slip velocity which in turn serves as the appropriate integrand to get the predicted pressure gradient between the two baroeffect bulbs.

III. OLIGOMERIC GAS STATES

Here the classic baroeffect calculation is extended to include gas aggregation. Aggregation into dimers and higher polymers is known to lead to anomalies in the temperature and concentration dependencies for the thermal diffusion (Soret) constant [18,19]. The order of gas polymers j increases for increasing pressure and increasing heavy gas content in a mixture; in contrast, increases in temperature tend to favor monomers over polymers. Dimerization occurs most frequently near the gas condensation point. Typical gas species known [17–19] to polymerize are Kr, Xe, Ne, and Ar. The existence of gas polymers has been demonstrated directly by means of mass spectrometry [21] and indirectly by pressure variations in the thermal diffusion (Soret) factor [17,19,22]. The use of the baroeffect experiment to elucidate aggregation states for gases as they approach their condensation point motivates the current work. Novel dynamics follow for baroeffect magnitudes which do not depend explicitly on molecular weight; in addition, the cases treated quantitatively prompt speculation regarding

possible complex and oscillatory diffusion.

As shown in Fig. 2, three cases will be treated here: (a) monomer counterdiffusing into j-mer; (b) arbitrary k-mer counterdiffusing into j-mer; and (c) arbitrary k-mer counterdiffusing into j-mer in the presence of a third, non-diffusing gas. For the third case, addition of a heavy gas which is uniformly distributed in both bulbs (and hence "nondiffusing") is known to suppress the baroeffect and lead to anomalous behavior in diffusive slip velocity near gas-capillary interfaces [16]. The fourth case (d) shown will be taken up qualitatively in Sec. VIII.

IV. PREDICTED BAROEFFECT RESULTS INCLUDING A MONOMER-POLYMER SYSTEM

The configuration for the baroeffect experiment is shown schematically in Fig. 2. Two gas bulbs, initially unconnected to each other, are filled to the same pressure with different gases. The two bulbs are subsequently connected by a capillary. As the gases counterdiffuse, any molecular weight difference between the two gas species translates into a faster average molecular velocity (and therefore diffusion) for the lighter gas. Hence the bulb initially filled with heavy gas shows a *transient pressure increase* owing to the greater mass influx of light gas. A second, wider tube, which remains blocked to mass flow (by a pressure gauge or liquid piston), measures the resulting pressure difference (or baroeffect) between the bulbs. The heavy-gas bulb always shows the higher transient pressure buildup, such that *a returning gas flow arises from heavy gas towards the lighter-gas bulb.* In particular, at low pressures ($\sim 0.1-1$ kPa), the pressure buildup equals 10% of the total pressure [9]. For typical binary systems (Ar-N_2, H_2-He, H_2-N_2), the baroeffect "is
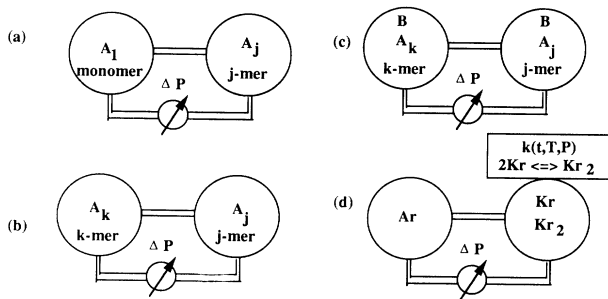

FIG. 2. Experimental schematic for the baroeffect setup. The blocked sidearm measures the pressure difference between the two bulbs. Pressure, p; temperature, T; and molecular weight, m. Cases treated include (a) monomer (light gas) and aggregated j-mer (heavy gas) of same molecular gas; (b) aggregated j-mer (light gas) and k-mer (heavy gas) of same molecular gas; (c) aggregated j-mer (light gas) and k-mer (heavy gas) in presence of third, nondiffusing component; (d) possible oscillatory case, with light gas (shown, argon) counterdiffusing into heavy gas (shown, krypton) which is capable of reversible dimerization with increased pressure. See Sec. VIII.

important even at quite high pressures (13.3 kPa). Accordingly, it is important to take it into consideration in a wide range of practical problems in gas dynamics" [4].

Expressions for pressure drop and isothermal diffusive slip velocity follow as a generalization of momentum-transfer arguments [9]. The diffusive slip velocity v_s appears as a linear extrapolation to the wall of two bulk velocities, the mass-averaged diffusion velocity v_m and gas velocity v_w, taken several mean free paths from the wall,

$$v_s = v_m - v_w \ . \tag{1}$$

At every point of solid contact, the usual no-slip condition requires fluid to stick. Using (1) this requires that a fluid's tangential surface velocity equals its near-wall gas velocity $v_s = v_w$ (such that $v_m = 0$ for a stationary wall).

The mass-averaged diffusion velocity equals

$$v_m = \frac{\sum\limits_{i=1}^{2} m_i n_i v_i}{\sum\limits_{i=1}^{2} m_i n_i} \ , \tag{2}$$

written in terms of species diffusion velocity v_i, molecular weight m_i, and moles n_i. The baroeffect experiment reaches steady-state diffusion, such that the net molecular flux vanishes

$$\sum_{i=1}^{2} n_i v_i = 0 \ , \quad n_1 v_1 = -n_2 v_2 = -D \frac{dn_1}{dy} \ , \tag{3}$$

where y is the distance along the capillary.

When written in terms of the binary diffusion coefficient D and the molar concentration gradient dn_1/dy, Eq. (2) reduces to

$$v_m = \frac{(m_2 - m_1)D \dfrac{dn_1}{dy}}{(n_1 m_1 + n_2 m_2)} \ . \tag{4}$$

Calculation of the near-wall gas velocity relies on three assumptions: (i) all molecules reach thermal equilibrium with the wall and hence depart with velocity v_w; (ii) an incoming number flux $\frac{1}{4}nc$ carries momentum flux $\frac{1}{4}mvnc$ towards the wall, such that (for simple molecules)

$$n_1 m_1 c_1 v_1 + n_2 m_2 c_2 v_2 = (n_1 m_1 c_1 + n_2 m_2 c_2)v_w \ ,$$

where c is the thermal speed and finally; (iii) equipartition of energy between isothermal species

$$\frac{c_1}{c_2} = \left[\frac{m_2}{m_1} \right]^{1/2} \tag{5}$$

such that

$$v_w = \frac{m_2^{1/2} - m_1^{1/2}}{\sum\limits_{i=1}^{2} n_i m_i^{1/2}} D \frac{dn_1}{dy} \ . \tag{6}$$

Hence, in the presence of an aggregated component, the expected pressure drop between light-gas bulb ($y=0$; $n_1, n_2 = 0$) and heavy-gas bulb ($y=L$; $n_2, n_1 = 0$) is

given by a Poisseiulle-type relation

$$\Delta p = \frac{8}{R^2} \int_0^L \eta v_w dx = -\frac{8\eta}{R^2} D \int_0^1 \frac{m_2^{1/2} - m_1^{1/2}}{n_1 m_1^{1/2} + n_2 m_2^{1/2}} dn_1$$

$$= \frac{8\eta D}{R^2} \ln j \ . \tag{7}$$

Here, $j = m_j / m_1$, or the oligomeric order of the aggregated, diffusing component and η is the averaged viscosity.

Thus in the limit of a monomer/(jth order oligomer) system (where $m_j = jm_1$), this pressure drop reduces to a baroeffect result which is independent of molecular weight and depends only on the aggregation state of the higher-order oligomer (Fig. 3). This closed analytical form has an appealing simplicity and (7) represents the primary result of this section.

As a further refinement, the molecular weight dependence of the diffusion coefficient can be approximated by the Chapman-Enskog form [17,18],

$$D = D_0 \left[\frac{m_1 + m_j}{2m_1 m_j} \right]^{1/2} = \frac{D_0}{(2m_1^{1/2})} \left[\frac{1+j}{2j} \right]^{1/2}, \tag{8}$$

where D_0 is the portion of the diffusion coefficient that is independent of molecular weight

$$D_0 = \frac{0.002\,68 T^{3/2}}{p \sigma_{12} \Omega_{12} T_{ij}^*} \tag{9}$$

and p is the average pressure, T is the temperature, and σ, Ω, and T_{ij}^* are the standard interaction terms. In the limit of large aggregation, $j \to \infty$, then the pressure change (7) varies as $(\ln j)$ and the inverse square root of monomer molecular weight $[\Delta p \sim (\ln j)/m_1^{1/2}]$. The predicted pressure change is shown in Fig. 3 for various molecular weights and gas aggregation states. For all molecular weights and mole fractions, the aggregation of
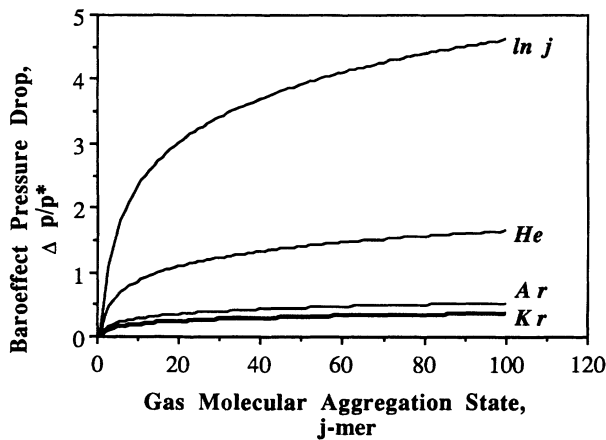

FIG. 3. The effect of gas aggregation state on predicted baroeffect pressure for different molecular weight gases (helium, argon, krypton). For the same aggregation, higher molecular weights suppress baroeffect. The pressure effect increases rapidly for low j-mers (from monomer to dimer, dimer to trimer) and approaches a limit for large j-mers. Experimental setup corresponds to Fig. 2(a).
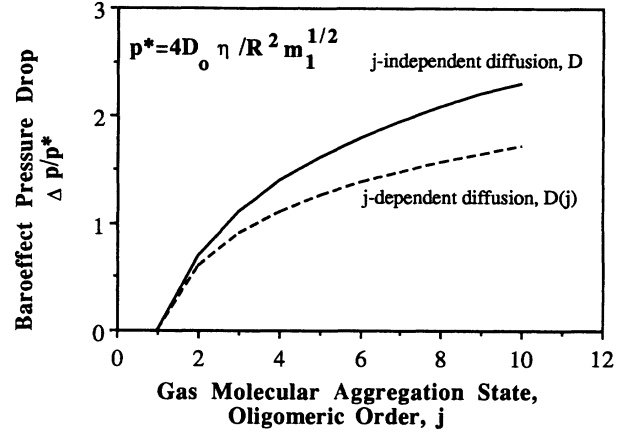

FIG. 4. Effect of aggregation state of j-mer on baroeffect, both for average diffusion coefficient (j independent) and for Chapman-Enskog diffusion (j dependent). Chapman-Enskog diffusion tends to reduce the predicted baroeffect for increasing aggregation of j-mer. Experimental setup corresponds to Fig. 2(a).

gas magnifies the baroeffect ($\Delta p \propto \ln j$). In the limit of all monomer ($j \to 1$), the pressure change vanishes ($\Delta p \to 0$). The dependence of the diffusion coefficient on the degree of polymerization j alters the expected baroeffect as shown in Fig. 4. The baroeffect is a maximum for an average diffusion coefficient which is j independent (such that Chapman-Enskog corrections always reduce the expected pressure gradient Δp).

V. DIFFUSIVE SLIP AND AGGREGATED GAS STATES

In the presence of an aggregated component, the diffusive slip velocity v_s follows from Eqs. (1), (4), and (6) as

$$v_s = MD \frac{dx_1}{dy} \ . \tag{10}$$

where both $M(j)$ and $D(j)$ are functions of aggregation state, and x_i is the mole fraction of component i ($n_i / \sum_i n_i$). For notational convenience, M corresponds to the mass-dependent portion of the velocity given by

$$M = \frac{m_2 - m_1}{x_1 m_1 + x_2 m_2} - \frac{m_2^{1/2} - m_1^{1/2}}{x_1 m_1^{1/2} + x_2 m_2^{1/2}} \ . \tag{11}$$

Equation (11) can be written in terms of the aggregation state by noting $m_j = jm_1$ and by le Chatelier's law [26],

$$x_1 = \frac{j}{j+1} \ , \quad x_{2\text{-}j\text{-mer}} = \frac{1}{j+1} \ .$$

Following tedious but straightforward algebra, the dependence of slip velocity on the aggregation state j follows from Eqs. (1), (6), and (10) as a complicated function of the oligomeric order j:

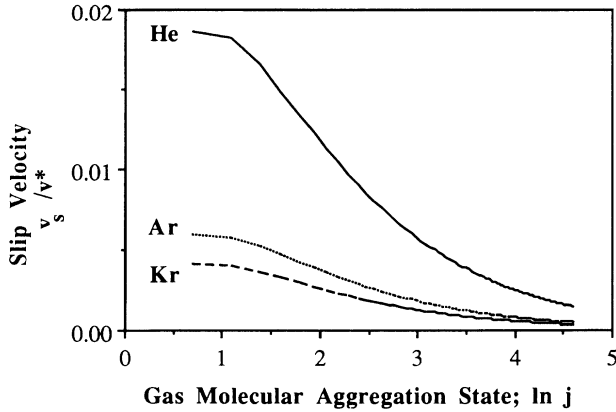$$M(j) = \frac{(j+1)[(j-1)(1+j^{-1/2}) - 2(j^{1/2}-1)]}{2j(1+j^{-1/2})} \ , \tag{12}$$

FIG. 5. Diffusive slip velocities as a function of heavy-gas aggregation (j-mer) for different molecular weight gases (helium, argon, krypton). Slip velocities decrease with increasing aggregation j and increasing molecular weight. Experimental setup corresponds to Fig. 2(a).

FIG. 6. Diffusive slip velocities as a function of light gas (krypton, j-mer) aggregation and relative aggregation ratio k/j. Slip velocities increase with increasing relative aggregation ratio k/j and decreasing absolute light-gas aggregation j. Experimental setup corresponds to Fig. 2(b).

which is shown in Fig. 5. It yields a positive slip velocity at the capillary wall which is always directed from heavy (j-mer) gas to lighter (monomer) gas for all j values. It is worth noting that (12) is independent of the specific molecular weights of the selected gas species and hence universal for all gases which aggregate into oligomers of jth order. For computational purposes, the least-squares fit to the discrete function equals $M(j)=0.87-0.40j$ (determination coefficient, $R=0.999$).

Combining the j dependence of the diffusion coefficient $D \propto [(1+j)/2j]^{1/2}$ with (12) and noting that

$$\frac{dx_1}{dy} = \frac{1}{(j+1)^2}\frac{dj}{dy} \qquad (13)$$

[where y is again the (long-axis) distance along the capillary], then one obtains the j dependence of the slip velocity. The function is plotted in Fig. 5, as normalized by $v^* = D_0 dj/dy$. As required, the velocity vanishes to give a no-slip condition for all monomer ($j=1$) in both bulbs [$v_s \rightarrow 0$ as $j \rightarrow 1$, since $M(j=1) \rightarrow 0$ in (12)].

VI. GENERALIZATION TO MIXED POLYMER SYSTEMS

The result for monomer/j-mer system can be generalized further to include two aggregation states (k-,j-mer) which counterdiffuse. If $\beta = k/j$ in Eqs. (6) and (7), the expected pressure change takes the form

$$\Delta p = \frac{4\eta D}{R^2}\ln\beta , \qquad (14)$$

which again is independent of specific molecular weight for an average diffusion coefficient D. Thus the baroeffect depends solely on the aggregation states (k,j).

From le Chatelier's law, $x_j = k/(j+k)$ and $x_k = j/(j+k)$, then the generalization of Eq. (12) for $M(\beta)$ is
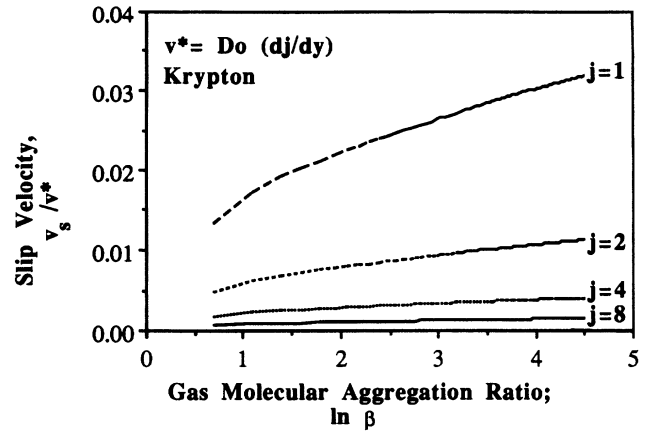
$$M(\beta) = \frac{(\beta-1)(\beta+1)}{2\beta} - \frac{(\beta^{1/2}-1)(\beta+1)}{(\beta^{1/2}+1)\beta^{1/2}} , \qquad (15)$$

which gives a slip velocity

$$v_s = D_0 M(\beta)\left[\frac{\beta}{2mj^3}\right]^{1/2}(1+\beta)^{-3/2}\left[\frac{dj}{dy}\right] . \qquad (16)$$

For the Chapman-Enskog form of the binary diffusion coefficient, (16) is dependent both on the relative (β) and absolute (j) aggregation in the gas, as well as monomer molecular weight m. The slip velocity is always positive for $k>j$, $\beta>1$ and is directed from the heavy gas (k) towards the light gas (j). For different values of light gas aggregation (j), slip velocities are shown in Fig. 6 for Kr. As the light-gas aggregation state j increases, the slip velocity decreases from its maximum at $j=1$.

VII. MIXED AGGREGATING BAROEFFECT INCLUDING A THIRD, NONDIFFUSING COMPONENT

The method developed previously can be extended to include two gases in different aggregation states (k,j) accompanied by a third, nondiffusing gas [16]. Since recent work [15] has suggested that wall-gas interactions may influence growth of high-quality optical films in microgravity, the ability to control diffusive slip by adding a third nondiffusing (and nonpolar) gas may prove interesting. As the composition of gas 3 is the same between the two bulbs, it is taken to be a nondiffusing component. If x_3 is the mole fraction of gas 3 and the molecular weight ratio of j-mer and gas 3 is $M = m_3/jm$, then the expected pressure change from Eqs. (7) and (14) is

$$\Delta p = \frac{8\eta D}{R^2}\ln\left[\frac{\beta^{1/2}+x_3(M^{1/2}-\beta^{1/2})}{1+x_3(M^{1/2}-1)}\right] . \qquad (17)$$

In the limit of no third gas, $x_3 \rightarrow 0$, then (17) reduces to the appropriate limiting form (7) for single species oligomers. For all aggregation order β, the presence of a third, nondiffusing component reduces the expected pressure change. This is shown for various molecular weights in Fig. 7.

As in the case for the pressure gradient, the presence of a third gas alters values for diffusive slip. As before, $M(\beta)$ is given by

$$M(\beta) = \frac{\beta - 1}{x_j + \beta x_k + M x_3} - \frac{\beta^{1/2} - 1}{x_j + \beta^{1/2} x_k + M^{1/2} x_3} . \quad (18)$$

The form of Eq. (18) introduces some additional physics into the problem. First, unlike the simple binary gas result, diffusive slip (9) including the third gas does not vanish in the limit of one highly aggregated gas $(\beta \rightarrow 0)$. Hence the presence of a third gas extends the finite diffusive slip region to include larger pressure drops expected for the gas system with larger relative aggregation. Moreover, unlike the binary result [9] in which diffusive slip is always directed from heavy to light gas, Eq. (18) introduces several distinct diffusive slip regimes. As indicated in Fig. 8 (for $n_j = n_k = n_3$), the molecular weights and aggregation states of the component gases determine the slip direction. In this case, the mole fractions are $x_j = \beta/(1 + \beta + k)$, $x_k = 1/(1 + \beta + k)$, and $x_3 = \beta j / (1 + \beta + k)$, where by definition $\beta j = k$. By solving for the zero crossings of Eq. (18), one finds (Fig. 8) the changes of direction for the diffusive slip velocity as a function of (k, j, M). Relative to the mass averaged velocity, slip can be positive, negative, or stagnant (no-slip).

In particular, slip velocities increase in a positive direction (i.e., in the direction of the mass-averaged velocity) for increasing molecular weight of the nondiffusing component (gas 3). For a given nondiffusing molecular weight M, no-slip occurs for a unique combination of ag-

FIG. 8. Three regimes for diffusive slip in the presence of a third, nondiffusing gas. Values for the slip velocity $[v_s/(D_0 dj/dy)]$ shown as a function of aggregation state of light gas j and the molecular weight ratio of nondiffusing component and j-mer $M = m_3/jm$. Parameter values, $\beta = 100$. Experimental setup corresponds to Fig. 2(c).

gregation states (j, β). Finally, negative slip occurs for increasing aggregation. (The physical interpretation given to negative slip has been discussed elsewhere [16]; it means that the wall velocity exceeds the mass-averaged velocity, a phenomenon somewhat akin to thermal [15] creep in various crystal-growth situations.) In general, diffusive slip velocity shows a marked dependence on the gas aggregation state.

VIII. DISCUSSION

The baroeffect is investigated here as a means to elucidate unknown gas aggregation states from measurements of the pressure gradient which evolves between two gas-filled bulbs. A number of cases have been examined and found to predict new flow regimes which depend on the gas's oligomeric order. Several problems remain. The interaction of aggregated gases with capillary walls is tractable, particularly for including some simple gas-wall collision physics at the boundary [27]. Solution aggregation states have previously been linked to crystal habit [26] and the analogous case for vapor crystal growth is approachable. Capillary-gas adsorption is an interesting model case for many heterogeneous processes generally, including catalysis and diffusion in porous media. In particular, laser action on the baroeffect is a further extension of the analysis with potential applications to surface treatments in the free-molecular regime [27].

As an initial treatment of the gas aggregation problem, the present work considered well-defined oligomeric or aggregation states only; the aggregation which offers more scientific importance, however, may be the time-dependent calculation for the condensation reaction [18] $R_j + R_k \rightleftharpoons R_i$, with equilibrium constant $k(p, T, t) = x_i/x_k x_j$. If this reaction has a pressure dependence, then interesting *oscillatory behavior* may be observable in both the reversible aggregation and *in the pressure*. This can be illustrated schematically as follows. Consider an
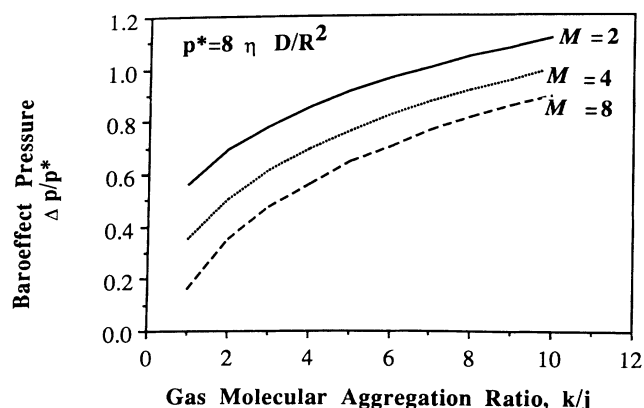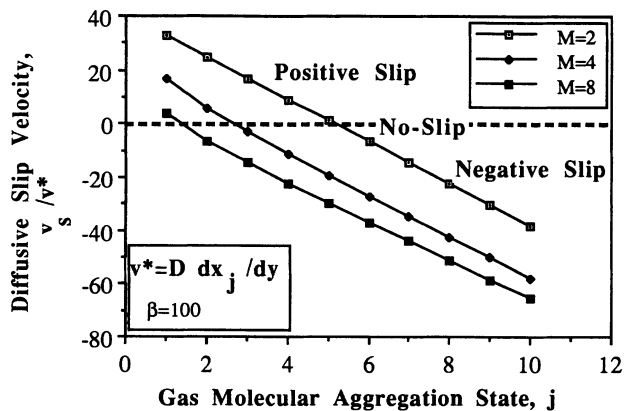

FIG. 7. Suppression of the baroeffect by addition of a third nondiffusing gas, with pressure change as a function of relative gas aggregation state k/j for counterdiffusing aggregates of j-mer and k-mer. Values are shown for ternary system, molecular weight ratio $M = m_3/jm$. For all aggregation values, increasing the molecular weight of the third gas suppresses the baroeffect, but less significantly for large mass differences between k-mer and j-mer. Experimental setup corresponds to Fig. 2(c).

argon-krypton system with krypton able to reversibly form dimers with an increase in pressure. Since krypton is heavier than argon, the transient pressure increase associated with the baroeffect of counterdiffusing argon will appear in the krypton-containing bulb. This pressure change leads to dimers of krypton and the question is posed: what effect does krypton aggregation have on the observed pressure change? There are two possibilities. Either the mole reduction upon dimerization will *reduce the pressure* in the heavy-gas bulb and thus *slow down the baroeffect,* or the opposing result, the increase in the relative molecular weight difference between krypton (upon partial dimerization) and argon will *increase the pressure driving force* between the two bulbs and hence *speed up the baroeffect.* In the first case, krypton aggregation reduces the molar pressure, while in the latter case, krypton aggregation increases the influx of argon due to the increased molecular weight difference between argon and

krypton dimers. The two counterbalancing effects may define a new steady equilibrium (in the presence of significant dissipation) or introduce possible oscillatory states wherein dimerization reversibly cycles between a maximum and minimum with varying pressure. The outcome will depend on the physical parameters of the particular gas experiment; however the possibility of observing complex (chaotic?) dynamics in a precise, but simple pressure experiment makes further pursuit of this question appealing.

It is worth noting that the more general measurement of a gas Kirkendall effect provides a particularly attractive experiment in microgravity [28,29]. With reduced convective flows owing to low gravity, gas buoyancy may not mix or mask the subtle effects of other bulk flows like Kirkendall effects. This approach may allow quantitative evidence for demonstrating such fundamental diffusion physics.

---

[1] K. P. McCarty and E. A. Mason, Phys. Fluids 3, 908 (1960). As widely cited in Soviet physics, the same experiment has been described using a variety of names: hydrodynamic flow, mass flow, nondiffusional flow, viscous bulk flow, the gas Kirkendall effect, and the Kramers-Kistemaker effect. In crystal growth, it most recently has been called concentration creep. In aerosols, related phenomena are called diffusion forces, diffusional slip, and diffusiophoresis. Of note, the baroeffect was the first experimental method used to determine diffusion coefficients (as opposed to trace diffusion coefficients) for isobaric and isothermal gases.

[2] R. B. Bernstein, J. Chem. Phys. 17, 209 (1949).

[3] B. V. Derjaguin and D. A. Batova, Dokl. Akad. Nauk SSSR 128, 323 (1959).

[4] P. V. Volobuev and P. E. Suetin, Zh. Tekh. Fiz. 35, 336 (1965) [Sov. Phys.—Tech. Phys. 10, 269 (1965)].

[5] L. Kotousov, Zh. Tekh. Fiz. 34, 2178 (1964) [Sov. Phys.—Tech. Phys. 9, 1679 (1965)].

[6] P. E. Suetin and P. V. Volobuev, Zh. Tekn. Fiz. 34, 1107 (1964) [Sov. Phys.—Tech. Phys. 9, 859 (1965)].

[7] L. S. Kucherov, R. Ya. Rikenglaz, Zh. Teor. Fiz. 36, 1758 (1959) [Sov. Phys.—JETP. 36, 1253 (1959)].

[8] N. D. Kosov and L. I. Kurlapov, Zh. Tekh. Fiz. 35, 2120 (1965) [Sov. Phys.—Tech. Phys. 10, 1623 (1966)].

[9] H. R. Kramers and J. Kistemaker, Physica, 10, 699 (1943).

[10] B. Opfell and B. H. Sage, Ind. Eng. Chem. 47, 918 (1955).

[11] G. S. Hartley and J. Crank, Trans. Faraday Soc. 45, 801 (1949).

[12] C. G. Ngan and E. B. Dussan, J. Fluid Mech. 209, 194 (1989).

[13] B. L. Markham and F. Rosenberger, Chem. Eng. Commun. 5, 287 (1980); D. W. Greenwell, B. L. Markham, and F. Rosenberger, J. Cryst. Growth 51, 413 (1981); B. L. Markham and F. Rosenberger, ibid. 67, 241 (1984).

[14] G. Mo and F. Rosenberger, Phys. Rev. A 44, 4978 (1991).

[15] D. E. Rosner, Phys. Fluids A 1, 11 (1989); D. E. Rosner and D. E. Keyes, NASA Report No. NAG3-898, 1988.

[16] D. A. Noever, Phys. Rev. Lett. 65, 1587 (1990).

[17] V. L. Zhadov, Sov. J. Eng. Phys. 35, 1126 (1978).

[18] K. E. Grew and W. A. Wakeham, J. Phys. B 4, 1548 (1971).

[19] W. A. Wakeham, J. Phys. B 4, 1564 (1971).

[20] B. P. Mathur and W. W. Watson, J. Chem. Phys. 51, 2210 (1969).

[21] R. Pedrys, Phys. Lett. 82A, 371 (1981); see also R. E. Leckenby and E. J. Robbins, Proc. R. Soc. London, Ser. A 291, 389 (1966).

[22] W. A. Oost and A. E. de Vries, Physica 41, 440 (1969).

[23] D. A. Noever, Phys. Lett. A 199, 253 (1990).

[24] D. A. Noever, J. Colloid Interface Sci. 147, 186 (1991).

[25] J. C. Maxwell, Scientific Papers (Dover, New York, 1962), Vol. II, p. 681; Philos. Trans. R. Soc. London 170, 231 (1879).

[26] P. G. Barber, J. Cryst. Growth 109, 99 (1991).

[27] D. A. Noever, Phys. Fluids A 2, 858 (1990).

[28] V. V. Levdanskii and O. B. Marynenko, Sov. J. Eng. Phys. 38, 301 (1980).

[29] Y. Malmejac and G. Frohberg, in Fluid Sciences and Materials Science in Space, edited by H. U. Walter (Springer-Verlag, Berlin, 1987), p. 188.